Time-Resolved Emission Spectroscopy of the Dansyl Fluorescence Probe†

Kenneth P. Ghiggino,‡ Anthony G. Lee,* Stephen R. Meech,§ Desmond V. O'Connor,§ and David Phillips§

ABSTRACT: Using a cavity-dumped laser system as the light source, we have recorded time-resolved fluorescence spectra for the dansyl group in a variety of systems. The fluorescence spectrum of dansylphosphatidylethanolamine incorporated into a variety of lipid bilayer systems at ambient temperatures shows very marked time dependence, with red shifts of up to 40 nm over a 40-ns period. Similarly, large red shifts are observed for dansylamide in 1-butanol at low temperatures, which can be tentatively attributed to the initial rapid formation of an intramolecular charge transfer state, followed by reorientation of the polar solvent molecules. The time-resolved behavior in the lipid bilayer system can, by comparison, also be at least partly explained by solvent reorientation, but the possibility of heterogeneity of the binding site must also be considered. The complex time dependence of the fluorescence of the dansyl group in these lipid bilayer systems considerably complicates the interpretation of fluorescence quenching and fluorescence energy transfer experiments.

Derivatives of the 5-amino-1-naphthalenesulfonates, particularly the dansyl (5-dimethylamino-1-naphthalenesulfonate) group, are used extensively as fluorescence probes of the structure and dynamics of biological macromolecules. They have been used in fluorescence quenching measurements and energy transfer studies, both as the donor (Marsh & Lowey, 1980) and as the acceptor (Haas et al., 1978; Fleming et al., 1979), and in the study of molecular motion by anisotropy decay measurements (Brochon & Wahl, 1972; Tawada et al., 1978; Wahl et al., 1978; Ikkai et al., 1979). These molecules have emission properties which are strongly dependent upon the nature of their environment; in particular, they exhibit a large red shift on going from a nonpolar to a polar environment. This property has commonly been used to study the "polarity" of binding sites in membranes and proteins (Leherer et al., 1981).

A number of studies, however, suggest that fluorescence in biological systems might be complex. Fluorescence emission normally occurs on a nanosecond time scale, whereas the relaxation of polar solvent molecules about the changed dipole moment of an excited state usually occurs in a few tens of picoseconds in fluid media (Halliday & Topp, 1978). Thus, solvent reorientation is complete before significant fluorescence emission occurs. This process is characterized by a large fluorescence Stokes shift with no corresponding change in the absorption spectrum. If, however, the fluidity of the medium is changed either by cooling the solvent or by incorporating the fluorophore into a different environment, such as a protein binding site, the environment may relax on the same time scale as the fluorescence decay of the molecule. This causes the spectrum to shift gradually to the red with time and yields complex, wavelength-dependent fluorescence decay kinetics. Such effects have been observed for a number of amino-naphthalenesulfonates (Chakrabarti & Ware, 1971; De Toma et al., 1976).

A further complication arises since it has been observed that 5-amino-1-naphthalenesulfonates exhibit a complex dependence of fluorescence lifetime and quantum yield on solvent polarity (Li et al., 1975). It has been suggested that an inversion of the two lowest excited singlet states may occur, depending upon the polarity of the solvent (Li et al., 1975). A further possibility is that a solvent/solute exciplex is initially formed prior to solvent relaxation (De Toma & Brand, 1977). In either case, it is clear that a change in the nature of the emitting state occurs on going from polar to nonpolar media and from fluid to glassy polar solvents.

With the availability of pulsed laser light sources, it is now straightforward to study time-dependent fluorescence processes in biological systems. We report here on our studies which show that the dansyl group exhibits extensive spectral shifts with time in both viscous polar solvents and when incorporated into biological membranes.

Experimental Procedures

Materials. Egg yolk phosphatidylcholine was obtained from Lipid Products Ltd., egg yolk phosphatidylethanolamine from Koch Light Ltd., and dansylphosphatidylethanolamine from Molecular Probes, Inc. Dansylundecanoic acid was prepared from dansyl chloride and aminoundecanoic acid.

Liposomes were prepared by codissolving lipid and probes in chloroform and drying onto the sides of flasks using a stream of dry nitrogen. Buffer (100 mM NaCl and 10 mM potassium phosphate, pH 7.2) was added to the flasks which were shaken to give a liposome suspension of 0.05 mg of lipid in 4 mL of buffer at a 100/1 lipid/probe ratio.

Dansylamide was recrystallized from ethanol. Butanol was dried with calcium hydride and fractionally distilled. For the low-temperature studies, the dansylamide concentration in 1-butanol was ca. 5×10^{-5} M. Temperature control was with an Oxford Instruments cryostat which was accurate to ±0.5 °C over several hours. This sample was degassed by six successive freeze–pump–thaw cycles. Other dansylamide/1-butanol samples were undegassed. An excitation wavelength of 300 nm and a spectral resolution of 1.5 nm were used throughout.

Methods. Total fluorescence spectra were recorded either on a home-built analogue spectrofluorometer or on the single photon counting equipment described below. In neither case are the spectra corrected for the wavelength response of the detector.

Time-resolved fluorescence measurements were made on an instrument which has been previously described (Ghiggino et al., 1980). Excitation is by the frequency-doubled output of a cavity-dumped Coherent-Radiation 590 dye laser operating with rhodamine 6G dye. This is driven by a Spectra-Physics

† From the Department of Biochemistry (A.G.L.) and the Department of Chemistry (K.P.G., S.R.M., D.V.O., and D.P.), The University of Southampton, Southampton, S09 5NH Hampshire, England. *Received December 9, 1980.* This work was supported by the Science Research Council, The Royal Society, and the University of Southampton.

‡ Present address: Department of Chemistry, Melbourne University, Parkville, Australia.

§ Present address: Davy Faraday Laboratory, The Royal Institution, London W1X 4BS, England.

0006-2960/81/0420-5381$01.25/0

166 4-W argon ion laser. The high, cavity-dumped, repetition rate (5 MHz) and laser intensity allows the rapid collection of fluorescence lifetimes with good signal to noise ratios and the rapid recording of time-resolved emission spectra.

The absolute reproducibility of the pulse shape enables accurate computational analysis of fluorescence decay curves. Data analysis was performed by using an iterative nonlinear least-squares reconvolution procedure (Bevington, 1969). The quality of the fit was judged by the value of the reduced χ^2 (χ^2_ν) and the distribution of the residual and autocorrelation of residual plots (Grinvald & Steinberg, 1974).

Time-Resolved Emission Spectra. There are two common methods of constructing time-resolved emission spectra using the single photon counting technique. In the first method, upper and lower level discriminators are set in the multichannel analyzer at voltages V_1 and V_2, corresponding to times t_1 and t_2 in the time to amplitude converter. This sets a gate width, δt ($=t_2 - t_1$), which discriminates against photons emitted outside that time range. This gate may be set at any time, Δt, after the onset of the rise of the excitation, which is taken as time equals zero. Photons arriving within this gate are spectrally analyzed by synchronizing the scanning speed of the monochromator with the channel advance rate of the multichannel analyzer, operating in the multichannel scaling mode, thus creating a time-resolved spectrum. In this method, the spectral resolution is set by the monochromator slit width and scanning speed. The time resolution is set by the gate width δt and the width of the excitation pulse.

The decay profile obtained in the single photon counting experiment [$I(t)$] does not represent the true decay of the sample but is a convolution of that decay with the excitation profile, or instrument response function [$P(t)$]. Thus

$$I(t) = \int_0^t P(t')G(t - t')\,dt'$$

where $G(t)$ represents the true decay of the sample. Hence, the time-resolved spectra obtained by the method outlined above, which are "time slices" of $I(t)$, are somewhat distorted by the excitation pulse (Easter et al., 1976; Meech et al., 1981). However, at very early times, with narrow gates, the excitation corresponds to a δ function, and at late times, its influence is negligible. Nevertheless, if qualitative data are to be obtained by analysis of the time-resolved spectra at intermediate Δt, this distortion must be removed.

A method of creating undistorted time-resolved spectra has been previously described (Easter et al., 1976; Meech et al., 1981). The function $I(t)$ is measured at a number of wavelengths across the fluorescence spectrum of the sample, and $G(t)$ is obtained by deconvolution (O'Connor et al., 1979; McKinnon et al., 1977). Convolved [$I(t)$] and deconvolved [$G(t)$] functions at two representative wavelengths are shown in Figure 1. Time-resolved spectra, $Y(\lambda,t)$, are then created by dividing the function $G(t)$, obtained at wavelength λ, by its calculated area, A, and multiplying by the intensity in the total fluorescence spectrum at the corresponding wavelength, $I(\lambda)$, that is

$$Y(\lambda,t) = \frac{I(\lambda)G(\lambda,t)}{A}$$

Thus, photons in discrete "time slices" are summed and arranged as a function of wavelength. In this method, spectral resolution is set by the number of decays obtained, and time resolution is limited only by the channel width in the multichannel analyzer.

Numerous problems are associated with obtaining $G(t)$ by deconvolution, particularly when physically significant decay parameters are required [see Wahl et al. (1974) for an example]. However, for the purpose described here, only an accurate representation of $I(t)$ is required, which is judged by the value of the reduced χ^2 (Bevington, 1969). In this case, $G(t)$ was chosen to be a sum of ten exponential terms, i.e.

$$G(t) = \sum_{i=1}^{10} A_i \tau_i$$

with the τ_i values being fixed and the A_i values as variable parameters (Ware et al., 1973). Fluctuations, sometimes observed at late times in such a function, were not seen in this case (Ware et al., 1973). When this function is inappropriate, a sum of three exponentials with both A and τ values freely varying is usually sufficient. The method is described in full in Meech et al. (1981).

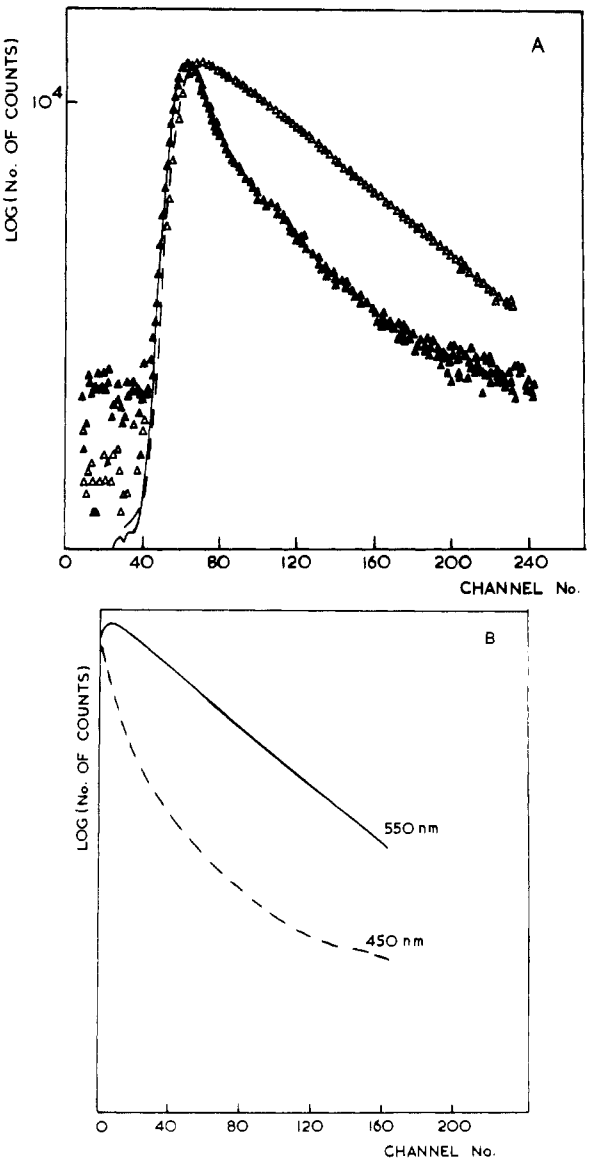

FIGURE 1: (A) Impulse response function at 450 (▲) and 550 nm (△). Solid (450-nm) and dashed (550-nm) lines represent the fitted (reconvolved) function. System: 1-butanol/dansylamide at 190 K, degassed one channel = 0.76 ns. (B) Deconvolved functions at 450 (---) and 550 nm (—); conditions as for Figure 1A.

Results

Model System: Time-Resolved Emission Spectroscopy of Dansylamide in 1-Butanol. Since the lipid bilayer provides a highly heterogeneous medium in which complex fluorescence properties are frequently observed (K. P. Ghiggino, D. Phillips, S. R. Meech, A. J. Roberts, A. G. Lee, R. Diggins, R. Sharma,

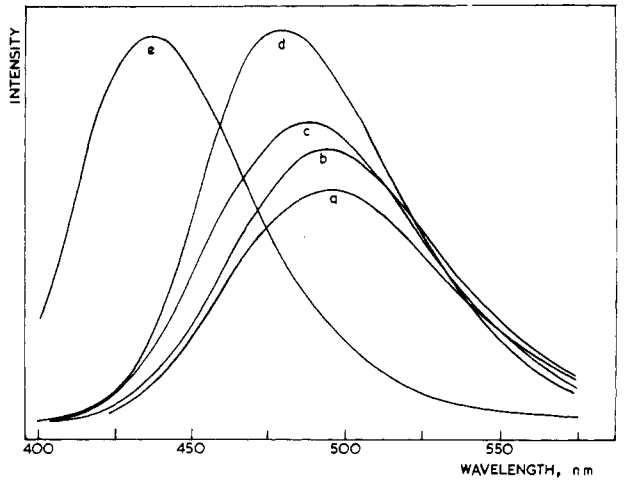

FIGURE 2: Temperature dependence of the total fluorescence spectra of dansylamide in degassed 1-butanol: (a) 280; (b) 220; (c) 190; (d) 160; (e) 85 K.

and M. Green, unpublished experiments), we initially studied the properties of the dansyl chromophore in a viscous polar environment.

Figure 2 shows steady-state fluorescence spectra of dansylamide in 1-butanol at various temperatures. A rather large shift occurs between the solid phase (85 K) and the "soft glass" (160 K), followed by a smaller red shift and decrease in intensity with increasing temperature. Figure 3 shows time-resolved spectra for this system at two temperatures and illustrates how the fluorescence emission spectrum shifts to the red at increasing times after excitation. These spectra were recorded directly as described above and are normalized to equal intensity at the peak maximum. The conventional fluorescence spectra of Figure 2 represent the sum over time of the time-resolved spectra, examples of which are shown in Figure 3. It is clear that at 190 K the fluorescence spectrum immediately after excitation ($\Delta t = 0$) is rather similar to the conventional fluorescence spectrum recorded at 85 K. With time, however, the spectrum shifts to the red and 23 ns after excitation has a peak maximum at 495 nm. At 235 K, the time-resolved behavior, while still present, is much less marked, presumably due to the greater solvent mobility at this temperature (Figure 3).

As has been described above, these time-resolved spectra are somewhat distorted by the excitation pulse, and Figure 4 compares spectra constructed from the convolved and deconvolved decays for early ($\Delta t = 3$ ns) and late ($\Delta t = 40$ ns) times. The differences are quite small, compared to the large shifts observed, and would only be important where quantitative data are required. It should be noted that even the deconvolved spectra are not totally free from distortions due to the wavelength dependence of the photomultiplier, which can be especially important on the rising edge of the decay curves (Wahl et al., 1974) and hence in spectra recorded at very early times. Since, using the direct method, time-resolved spectra can be recorded in ca. 30 min, whereas the deconvolved spectra require very considerable computation time, the direct recording method has proved to be the most useful, for qualitative data.

Representative fluorescence decays for dansylamide in 1-butanol at 190 K were analyzed by conventional methods, being fitted to one-, two-, and three-exponential functions. The data obtained from these analyses are presented in Table I. It is immediately clear that the fluorescence decay in viscous media is wavelength dependent and cannot be described by any simple kinetic model. The very poor fits to a two-exponential function and the variation of the fitted decay times

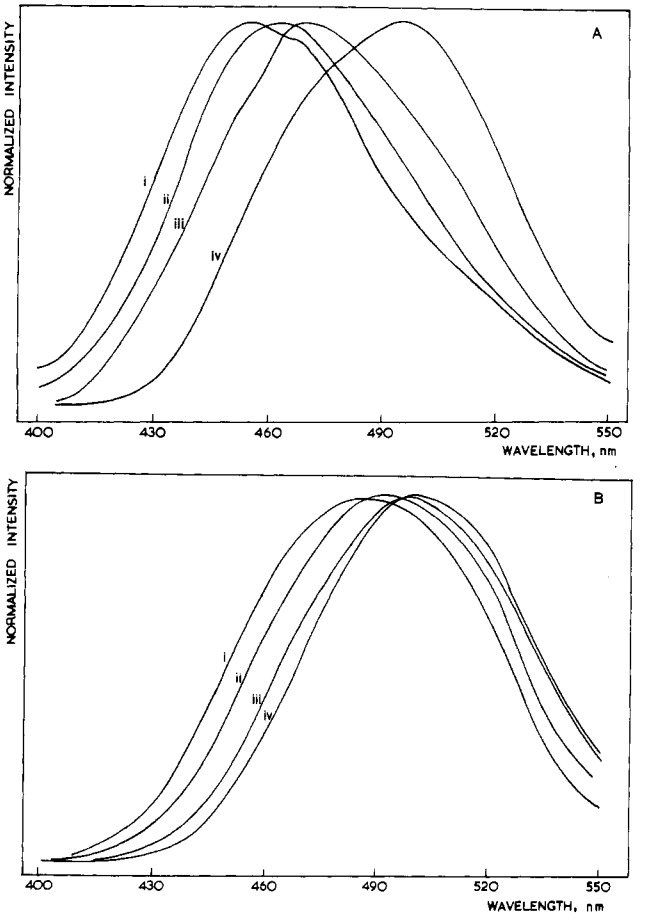

FIGURE 3: (A) Convolved time-resolved emission spectra of dansylamide in 1-butanol at 190 K (undegassed): (i) $\Delta t = 0$ ns, $\delta t = 4.5$ ns; (ii) $\Delta t = 3.3$ ns, $\delta t = 3.3$ ns; (iii) $\Delta t = 8.8$ ns, $\delta t = 3.8$ ns; (iv) $\Delta t = 23.0$ ns, $\delta t = 4.5$ ns. (B) Convolved time-resolved emission spectra of dansylamide in 1-butanol at 235 K (undegassed): (i) $\Delta t = 0$ ns, $\delta t = 4.5$ ns; (ii) $\Delta t = 3.3$ ns, $\delta t = 3.3$ ns; (iii) $\Delta t = 8.4$ ns, $\delta t = 2.6$ ns; (iv) $\Delta t = 26.3$ ns, $\delta t = 4.5$ ns.

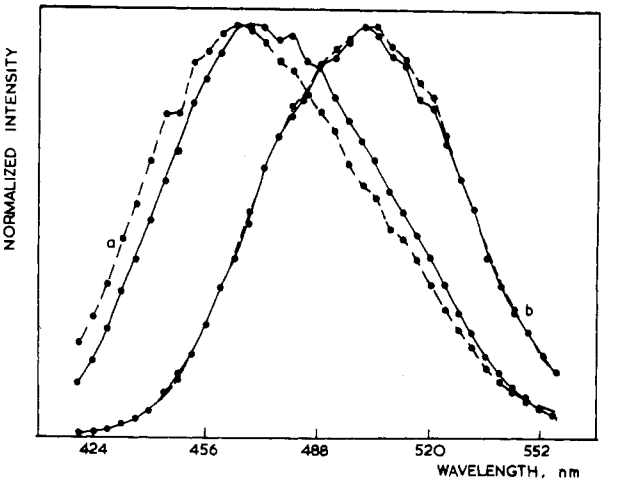

FIGURE 4: Comparison of time-resolved emission spectra of dansylamide in 1-butanol at 190 K (degassed), constructed from convolved (---) or deconvolved (—) decays: (a) $\Delta t = 3$ ns; (b) $\Delta t = 30$ ns.

across the emission spectrum rule out the possibility of excimer/exciplex formation being the mechanism of the red shift. The decay is reasonably well described by a fit to a three-exponential function, but, as stated previously, we are reluctant to attach any meaning to the numerical results obtained.

When the decays are analyzed on the red edge of emission (500–550 nm), a strong component with a negative preexponential factor is required to describe the data, suggesting that

Table I: Fluorescence Decay Kinetics of Dansylamide in 1-Butanol at 190 K

fitted function	wavelength (nm)	A_1[a]	τ_1 (ns)	A_2	τ_2 (ns)	A_3	τ_3 (ns)	χ^2_ν[b]
single exponential	420		3.38 (0.01)[c]					86.1
	460		12.11 (0.02)					124.5
	500		20.41 (0.02)					5.4
dual exponential	420	0.44	2.38 (0.01)	0.01	15.36 (0.01)			10.3
	460	0.18	6.07 (0.05)	0.05	19.93 (0.10)			2.2
	500	0.13	18.60 (0.12)	0.03	25.71 (0.34)			4.1
triple exponential	420	0.50	1.79 (0.03)	0.05	7.44 (0.17)	0.001	56.10 (3.2)	1.2
	460	0.13	4.31 (0.30)	0.08	10.01 (0.83)	0.034	22.21 (0.5)	1.3
	500	0.06	14.38 (0.38)	0.05	22.32 (0.98)	0.060	22.35 (0.8)	1.6

[a] Preexponential factor. [b] Reduced χ^2. [c] Numbers in parentheses indicate standard deviations.

the red-shifted components are being created by a means other than direct excitation. This is also seen in the deconvolved function of the 540-nm decay (Figure 1B), where an initial rise in the intensity vs. time profile is observed. When the same decays are analyzed only at late times, i.e., ignoring the first part of the decay, a good fit to a single exponential function is obtained; for example, at 540 nm, τ = 21.91 ns and χ^2_ν = 1.2. These results are consistent with a continuous relaxation process occurring on a time scale comparable to that of fluorescence decay. As described later, the initial rise, observed on the red edge, provides a means for distinguishing between static and dynamic processes in lipid systems.

No further red shift of the deconvolved time-resolved emission spectra is observed at times later than 60 ns after excitation. Thus, at this time, we are probably observing the spectrum of the totally relaxed species, and the single-component decay obtained when the first part of the decay (i.e., the first 7.6 ns) is ignored probably corresponds to the decay of the totally relaxed species.

In contrast to the complex behavior in viscous polar solvents, the behavior in fluid polar media is simpler. Thus, in methanol at 290 K, the fluorescence decays are well fitted to single-exponential decay kinetics over the whole of the fluorescence spectrum, with τ = 17.99 ns (χ^2_ν = 1.08). At 280 K in 1-butanol, no time-resolved spectral behavior is observable, but, although a reasonable fit to a single exponential is observed, the high χ^2_ν value (= 1.8) suggests that there is still a small contribution from some unrelaxed components.

The convolved time-resolved spectra shown in Figure 3 establish that the red shift is due to a continuous relaxation phenomenon. That is, the spectra shift continuously toward lower energy as the time gates are set at progressively later times. Comparison of the 235 and 190 K results further shows that this shift is dependent on the rigidity of the environment. The early time spectrum at 190 K shows a blue-shifted emission which is almost wholly absent at 235 K. Spectral data for temperature dependence of the total fluorescence spectra are presented in Table II.

It is immediately noticeable (Figures 3 and 5) that the spectral shift is accompanied by changes in the bandwidth of the time-resolved spectra. The spectrum at time equals zero is rather narrow, whereas those at intermediate times are quite broad. At later times, as the emission shifts further to the red, the spectra again become quite narrow (Figure 5). This is inconsistent with a simple solvent relaxation mechanism. The possible origins of this behavior will be discussed later.

Since fluorescence spectra of biological systems are usually recorded under undegassed conditions, we have also studied the effect of degassing on the spectra of dansylamide in 1-butanol. At 280 K, no differences were observable in the maxima and bandwidth of the total fluorescence spectra

Table II: Total Fluorescence Spectra

system	temp (K)	λ_{max} (nm) (±1 nm)	fwhm (nm)[a]
dansylamide/ 1-butanol, undegassed	280	494	78
	235	496	80
	220	493	84
	190	482	80
	160	455	74
	130	442	64
	85	440	56
dansylamide/ 1-butanol, degassed	280	496	76
	235	494	80
	220	493	80
	190	487	83
	160	481	73
	130	437	65
	85	437	64

[a] Full width at half-maximum height (±2 nm).

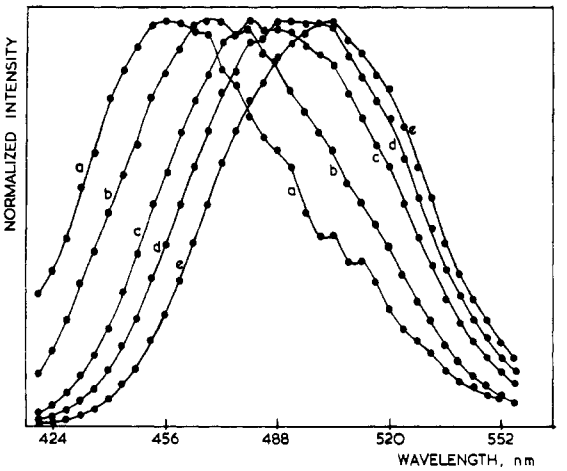

FIGURE 5: Deconvolved time-resolved emission spectra of dansylamide in 1-butanol at 190 K (degassed): (a) Δt = 0; (b) Δt = 3; (c) Δt = 9.1; (d) Δt = 18.2; (e) Δt = 48.6 ns. δt = 0.76 ns throughout.

whether or not the sample was degassed (Table II). At intermediate temperatures (235–160 K), however, the undegassed sample exhibits fluorescence which is to the blue of that observed for the degassed sample. This effect is also apparent in the time-resolved spectra. The Δt = 0 spectra, degassed or undegassed, at 190 K have the same value of λ_{max}, whereas 9 ns after excitation the spectrum of the degassed, deconvolved, emission is 14 nm to the red of that of the undegassed sample. The undegassed time-resolved spectra were obtained by the direct (gated) method. However, this shift is not wholly associated with the distortion mentioned previously since the spectrum constructed from undeconvolved decays, of the degassed sample, 9 ns after excitation is also to the red of that

Table III: Spectral Data for Dansyl Probes in Lipid Bilayer Systems

system		Δt (ns)	δt (ns)	λ_{max} (nm)	fwhm (nm)[a]
dansylphosphatidyl-ethanolamine/egg phosphatidylcholine (1/100)	EGS[b]	0.0	7.7	495	91
	LGS[c]	42.2	15.4	505	72
	TFS[d]			503	70
dansylphosphatidyl-ethanolamine/egg phosphatidylcholine/ cholesterol (1/100/ 100)	EGS	0.0	6.4	477	121
	LGS	42.2	12.8	517	64
	TFS			513	78
dansylphosphatidyl-ethanolamine/ phosphatidyl-ethanolamine (1/100)	EGS	0.0	8.4	485	121
	LGS	42.2	13.4	513	68
	TFS			510	74
dansylundecanoic acid/egg phospha-tidylcholine (1/ 100)	EGS	0.0	8.7	515	90
	LGS	31.4	15.3	518	78
	TFS			517	80

[a] See footnote *a* of Table II. [b] Early-gated (undeconvolved) time-resolved emission spectrum. [c] Late-gated (undeconvolved) time-resolved emission spectrum. [d] Total fluorescence (time-integrated) spectrum.

observed for the undegassed sample. Time-resolved spectra obtained (from the degassed sample) in this way should be comparable to those obtained from the gated method. However, the maxima for spectra obtained from undeconvolved decays are difficult to measure since these tend to suffer from poor signal to noise properties (Meech et al., 1981).

The oxygen quenching results show that a distribution of decay times exists when dansylamide is dissolved in a viscous polar medium, with the longer lived species being preferentially quenched in a diffusion-controlled process. The blue shift observed when a quencher is added suggests that the longer lived components emit to the red of the spectrum. This is consistent with theoretical models for solvent relaxation about the altered dipole moment of an excited state (Bakhshiev et al., 1966; Rapp et al., 1971). These results are consistent with the observed time-resolved spectra and complex fluorescence decay kinetics which exhibit a longer mean liftime on the red edge of the emission (Figure 1).

Lipid-Probe System. Detailed study of a heterogeneous system such as a lipid/water system is considerably more difficult than a simple solute/organic solvent system. We chose to study dansylphosphatidylethanolamine incorporated into various liposome systems, since there would be no problem of partitioning of the probe between aqueous and lipid phases. The conventional fluorescence spectra of dansylphosphatidylethanolamine incorporated into liposomes (see Figure 6 and Table III) show a relatively blue-shifted emission, so that the dansyl group must be "folded back" in some way from the head group of the lipid into a more nonpolar region of the lipid bilayer. In such a system, if we were to see time-resolved fluorescence behavior at ambient temperatures, there would be two likely explanations. (i) *Static.* The dansyl group is positioned at a variety of sites within the lipid bilayer, each with different fluorescence decay times and different fluorescence maxima. (ii) *Dynamic.* Either solvent reorientation of the type described in 1-butanol at low temperature is occurring or the dansyl group is moving between different environments on the fluorescence time scale, or a combination of the two.

Figure 6 shows undeconvolved time-resolved spectra for dansylphosphatidylethanolamine incorporated into liposomes

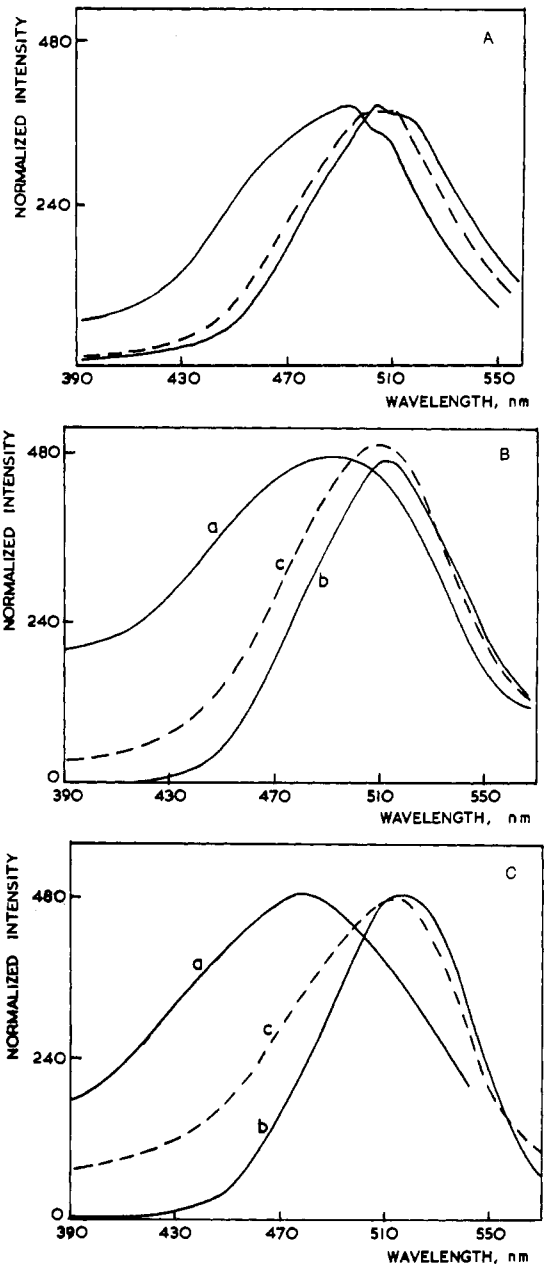

FIGURE 6: Comparison of time-resolved emission spectra of dansylphosphatidylethanolamine in lipid systems, showing early- and late-gated emissions (—) and the total fluorescence spectra (---). For gate settings, see Table III. (A) Dansylphosphatidylethanolamine incorporated into egg yolk phosphatidylcholine. (B) Dansylphosphatidylethanolamine incorporated into egg yolk phosphatidylcholine/cholesterol (1/1). (C) Dansylphosphatidylethanolamine incorporated into egg yolk phosphatidylethanolamine.

of egg yolk phosphatidylcholine at a 100/1 lipid/probe ratio. It is clear that shifts of the spectra with time do indeed occur. The late-gated spectrum can be considered as the true spectrum since the effect of convolution with the excitation pulse at these times will be negligible. The early-gated spectra will be somewhat distorted by the excitation profile because of the widths of the gates which were required to give good signal to noise ratios. This distortion will, however, be small when compared to the magnitude of the shifts observed. The spectral data are presented in Table III.

Analysis of the decays again yields complex, wavelength-dependent, fluorescence lifetimes which are described by a minimum of two and more usually three components (Table IV). In common with the model system, a negative component was required to fit the data obtained on the red edge of the

Table IV: Fluorescence Decay Kinetics of Dansylphosphatidylethanolamine in Lipid Systems at 25 °C

system	fitted function	wavelength (nm)	A_1[a]	τ_1, ns	A_2	τ_2 (ns)	χ^2_ν[b]
egg yolk phosphatidylcholine	single	450		5.45 (0.02)[c]			58.6
		485		9.39 (0.03)			23.4
		570		14.13 (0.04)			16.9
	double	450	0.99	2.71 (0.07)	0.01	10.47 (0.24)	2.2
		485	0.05	3.43 (0.20)	0.03	11.71 (0.19)	2.3
		570	0.04	4.42 (0.44)	0.07	12.25 (0.19)	3.8
egg yolk phosphatidyl-ethanolamine	single	450		5.07 (0.02)			88.0
		485		9.65 (0.03)			34.0
		570		14.5 (0.04)			9.9
	double	450	0.11	2.24 (0.05)	0.02	9.99 (0.17)	2.1
		485	0.05	3.23 (0.16)	0.03	12.3 (0.17)	3.1
		570	0.02	4.15 (0.58)	0.06	13.2 (0.18)	3.8
egg yolk phosphatidylcholine/ cholesterol (1/1)	single	450		6.56 (0.03)			128.0
		485		11.39 (0.04)			32.0
		570		15.01 (0.05)			11.2
	double	450	0.12	2.17 (0.05)	0.02	12.77 (0.19)	1.6
		485	0.05	2.34 (0.14)	0.04	13.53 (0.12)	1.4
		570	0.03	2.25 (0.28)	0.06	13.90 (0.09)	1.3
dansylundecanoic acid/egg yolk phosphatidylcholine	single	460		7.23 (0.01)			180.0
		490		12.20 (0.02)			93.0
		550		13.24 (0.02)			70.0
	double	460	0.28	3.00 (0.02)	0.04	14.42 (0.09)	2.55
		490	0.15	4.31 (0.05)	0.09	16.23 (0.08)	1.85
		550	0.12	7.08 (0.04)	0.07	19.00 (0.08)	10.2

[a] Preexponential factor. [b] Reduced χ^2. [c] Numbers in parentheses indicate standard deviation.

emission spectrum. These results are qualitatively comparable to those obtained for the model system.

The results suggest that some dynamic motional process is responsible for at least part of the observed red shift. This would imply that the dansyl group is exposed to a polar environment (water or polar groups in the lipid head group) within its fluorescence lifetime, as only some interaction with a polar medium can give rise to such effects.

If the motional process were the movement of the dansyl groups between different environments, then the motion would have to be to an environment of greater polarity in order to produce a red shift. This would, in fact, occur due to the greater polarity of the excited state of the dansyl group. Diffusion from polar to nonpolar sites would be equivalent to an energetically unfavorable "antirelaxation".

On addition of cholesterol (Figure 6B), both the late-gated and the total fluorescence spectra undergo shifts to the red, whereas the early-gated spectrum undergoes a substantial blue shift when compared to liposomes of phosphatidylcholine in the absence of cholesterol.

We interpret this result as being due to two effects. First, cholesterol reduces the amount of the dansyl group in the less polar environments, as a result of incorporation of cholesterol into the nonpolar regions of the bilayer. Second, cholesterol reduces the rate of motion within these less polar regions.

The first factor will produce a red shift of the total fluorescence spectrum. An alternative explanation of the red shift, that it is due to a more rapid environmental relocation in the presence of cholesterol, is, we feel, unlikely due to the known effectiveness of cholesterol in reducing mobility within the lipid bilayer (Lee, 1978).

The second factor will produce a blue shift in the early-gated spectrum, as can be seen from the results in 1-butanol, where a reduction in temperature causes a large blue shift for the early-gated spectra (Figure 3). An alternative explanation is that the blue shift of the early-gated spectrum, in the presence of cholesterol, is caused by a displacement of the dansyl groups, already in relatively nonpolar sites, to even less polar sites, presumably nearer the center of the bilayer. This we consider unlikely since the rigid sterol ring of cholesterol extends down to about C11 of the lipid fatty acyl chains (Stoffel et al., 1974), and from molecular models, it seems unlikely that the dansyl group in dansylphosphatidylethanolamine could penetrate the bilayer as far as this.

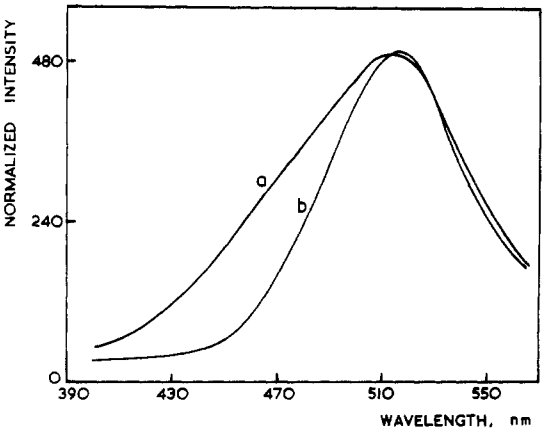

FIGURE 7: Time-resolved emission spectra of dansylundecanoic acid incorporated into egg yolk phosphatidylcholine: (a) Δt = 0 ns, δt = 8.7 ns; (b) Δt = 31.4 ns, δt = 15.3 ns.

For dansylphosphatidylethanolamine incorporated into liposomes of egg yolk phosphatidylethanolamine, the fluorescence behavior is intermediate between the cases of phosphatidylcholine with and without cholesterol. This is consistent with the known higher density of packing in bilayers of phosphatidylethanolamines (Michaelson et al., 1974).

We have also studied dansylundecanoic acid incorporated into liposomes of egg yolk phosphatidylcholine. Again complex, wavelength-dependent, fluorescence decays are observed. In the time-resolved spectra (Figure 7), the spectral maxima of early, late, and conventional fluorescence spectra are nearly coincident. Nevertheless, there is a marked broadening to the blue observed in the early-gated time-resolved spectrum. It could well be that this represents blue-shifted components which are incompletely resolved because of the wide time gate (9 ns) necessary to record reasonable spectra.

Discussion

Most analyses of fluorescence data in biological systems assume that the fluorescence decay can be fitted by a simple functional form and that fluorescence spectra do not change with time after excitation. We have shown that neither of these are true for the dansyl group when incorporated into lipid bilayers. The complex fluorescence phenomena described above, which may be observed either in systems of high viscosity or where a heterogeneity of binding sites is possible, can have a considerable effect on the interpretation of many of the fluorescence measurements carried out on biological systems. For example, fluorescence quenching is often used to test accessibility of groups in proteins to quenching agents. If the fluorescence probe being studied shows time-resolved behavior, then the spectrum will be shifted to the blue due to preferential quenching of the longer lived emission, as shown by the oxygen quenching results presented here. This will lead to nonlinear Stern–Volmer plots and possible errors in the calculation of numbers of exposed groups etc.

In the measurement of distance by fluorescence energy transfer efficiency, the value of the overlap integral I, where

$$I = \int_0^\infty \delta D_*(\nu)\epsilon_A(\nu)\, d\nu/\nu^4$$

and $\delta D_*(\nu)$ is the fluorescence spectral distribution of the donor and $\epsilon_A(\nu)$ is the extinction coefficient of the acceptor as a function of the frequency, ν (cm^{-1}), will depend upon the state of relaxation of the system and may change during the lifetime of the fluorescent state. This will be important when the donor exhibits time-resolved emission properties. The system of choice for energy transfer measurements would thus be of the type naphthalene donor and aminonaphthalene acceptor (Haas et al., 1978). Under these conditions, the required measurements would be made on the naphthalene chromophore which does not exhibit such complex behavior.

In fluorescence anisotropy measurements, as well as in the above cases, it is generally assumed that both k_F, the radiative transition probability, and Φ_F, the quantum yield, are constants. This may not be the case for the probes considered here when incorporated into a rigid polar environment since it seems that the nature of the emitting state is changing with time. If this is the case, then the angle between the absorbing and emitting dipoles may also be time dependent which will clearly affect fluorescence anisotropy measurements.

Although the time-resolved behavior of the type observed for the dansyl group will complicate many analyses of fluorescence data, it could also be of potential use, since it means that fluorescence spectra are dependent both on polarity and on fluidity. In order to exploit this motional information, it is necessary to develop a model for the fluorescence behavior of the dansyl group. Others (De Toma et al., 1976; Gafni et al., 1977) have analyzed time-resolved spectra according to the model of Bakhshiev et al. (1966). In this model, the decay of the sample at energy ν (cm^{-1}), $I(\nu,t)$, is represented as being the product of an electronic decay term, $i(t)$, and a spectral shift term, $\delta(\nu,t)$, which may be obtained from the time-resolved spectra (De Toma et al., 1976; Gafni et al., 1977), namely

$$I(\nu,t) = i(t)\delta(\nu,t)$$

If assumptions about the electronic decay of the molecule (that quantum yield and radiative transition probability are independent of the state of relaxation) are valid, then $i(t)$ should be recoverable as a monoexponential function. This is not the case for dansylamide in 1-butanol, which suggests that the above assumptions may be invalid. This contention is supported by the observation that the deconvolved spectrum at $\Delta t = 0$ is narrower than that found 3 ns after excitation (Figure 5, Table II). This suggests that a rapid change occurs in the nature of the emitting state, prior to solvent relaxation. This is also evident from the temperature dependence of the total fluorescence spectra (Figure 2), which shows a very large shift in the temperature region where the motion of the solvent molecules would be quite restricted (85–160 K). It is clear from these results that some other process is occurring on a more rapid time scale than solvent reorientation and is responsible, at least in part, for the observed red shift.

The nature of this fast process has not, as yet, been fully characterized. It has been observed that a change in the nature of the emitting state occurs, for 5-dimethylaminonaphthalene and related compounds, on going from a nonpolar to a polar environment (Li et al., 1975) as well as on going from the glass to the fluid state as observed here. This has been assigned as a level inversion of the first two excited singlet states of the 5-aminonaphthalene (which are close in energy), in polar solvents. The relative contribution from the charge transfer configuration in the description of these two states implies that S_2 (^1L_a in Platt notation) has a larger dipole moment than S_1 (^1L_b). Thus, in a polar solvent, the ^1L_a state interacts more strongly with the medium than does the ^1L_b state. Hence, relaxation of the solvent cage may lower the energy of the ^1L_a state below that of the ^1L_b state such that, in polar solvents, the fluorescence emission is from the ^1L_a state (Mataga, 1963; Li et al., 1975). This mechanism describes qualitatively the observed behavior. However, it does still require the dipolar reorientation of a solvent shell.

It has also been noted that 2-anilinonaphthalene, the fluorescence of which is strongly dependent upon solvent polarity, forms a stoichiometric exciplex with alcohols in cyclohexane solution (De Toma & Brand, 1977). The emission spectrum of 2-anilinonaphthalene in cyclohexane, when less than 1% alcohol (by volume) is present, is substantially red shifted from the pure cyclohexane solvent emission spectrum. At these low alcohol concentrations, the formation of a solvent shell is unlikely; thus, the observed red shift cannot be due to a solvent relaxation mechanism. It should, however, be noted that there is a substantial difference between the electronic structures of the 1- and 2-substituted naphthalenes (Nishimoto & Fujishiro, 1964; Nishimoto, 1969). Also, self-association of alcohols in hydrocarbon solvents may create localized regions of a high dielectric constant, which may complicate the observations.

The results presented here suggest that a different mechanism for the red shift of 5-amino-1-naphthalenesulfonate derivatives, in polar solvents, is required. The time-resolved spectra establish that the red shift is a solvent relaxation phenomenon but also that a change in the nature of the emitting state occurs between the Franck-Condon initially excited state and the final, solvent-relaxed state. This is also seen in the changing bandwidths of the temperature-dependent total fluorescence spectra (Figure 2). The large red shift between 85 and 160 K suggests that this change in emitting state occurs on a time scale somewhat faster than that of conventional dipolar reorientation. This may explain the observation that the rate of solvent relaxation, as shown by time-dependent spectral shifts, is significantly faster than that expected from the solvent dielectric relaxation time though other effects may be important (Ware et al., 1971).

It is not the purpose of the present work to establish definitely the origin of this fast process; however, one possible

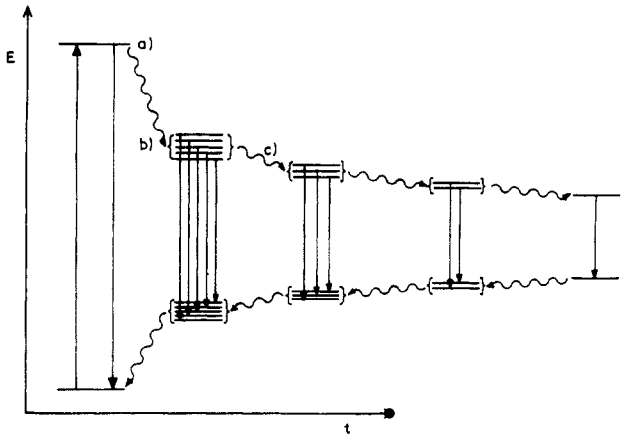

FIGURE 8: Diagrammatic representation of relaxation processes. (a) Initially excited Franck-Condon state; (b) postulated charge transfer state; (c) relaxation of solvent dipoles. Solid lines indicate absorption and fluorescence; wavy arrows indicate a relaxation process; other radiationless processes are not included.

explanation is that intramolecular charge transfer in the initially excited Franck-Condon state, presumably from the nitrogen lone pair to the naphthalene π-electron system, is enhanced by the presence of polar solvent molecules. Such charge transfer would be more favored if the amino group adopts a different configuration in the excited state [see Lipinski et al. (1980) for an example]. Further work on the origin of the postulated, charge transfer state is in progress.

The substantial narrowing of the time-resolved spectra in the single solvent system over the period Δt = 3–60 ns may be explained as follows. In the ground state, the solvent cage will adopt a more or less random configuration about the chromophore. In the excited state, there will be a preferred orientation of solvent dipoles about the postulated, rapidly formed, intramolecular charge transfer state. Hence, at early times, the fluorophore will experience a random distribution of environments, resulting in a broad spectral distribution. The least favorable solvent/solute configurations will decay quite rapidly; hence, at somewhat later times, the environment will be more ordered, and a narrower spectrum will result. The spectral characteristics observed for the dansyl chromophore in a single environment are summarized in Figure 8.

In extrapolating from the case of dansylamide in 1-butanol to that of the dansyl group incorporated into lipid bilayers, it is necessary to consider the possibility that the dansyl group might occupy more than one type of site within the bilayer, thus exhibiting complex fluorescence characteristics because of this heterogeneity. However, a static distribution of sites cannot explain all of the observed fluorescence phenomena. Fluorescence decays recorded at the red edge of the spectrum exhibit a rise time which must result from dynamic processes (Figure 1B). These dynamic processes we picture as being either motion of polar molecules (water, lipid head group, glycerol backbone, etc.) about the dansyl group or movement of the dansyl group between sites (see Results). In simple organic solvents at room temperature, motion of the solvent is fast on the fluorescence time scale so that fluorescence spectra are insensitive to the rate of this motion. However, on being cooled to near the glass transition, the time scales of motion and fluorescence become comparable, and changes in the rates of motion produce large changes in the fluorecence spectra (Figure 2). Since we see motional effects in the fluorescence spectra of lipid bilayer systems, the implication is that the rates of motion are more comparable to those of a glass than of a fluid organic solvent system.

We conclude, therefore, that both environmental relaxation and multiple siting may be responsible for the time-resolved behavior observed for the dansylphosphatidylethanolamine probe in lipid systems. It has not, as yet, proved possible to assess the relative importance of those two mechanisms to the observed time-resolved behavior. Further work is in progress using both deconvolved time-resolved emission spectra and differential quenching techniques (K. P. Ghiggino, D. Phillips, S. R. Meech, A. J. Roberts, A. G. Lee, R. Diggins, R. Sharma, and M. Green, unpublished experiments).

With the current availability of pulsed laser systems, it is likely that time-resolved fluorescence studies of biological systems will become fairly routine. Such methods will be necessary to obtain accurate data for many quenching and energy transfer experiments. We are currently analyzing the kind of inaccuracies that can arise when time-dependent shifts of spectra are ignored in such studies. It is also clear that very large shifts in fluorescence spectra can occur for probes bound to different sites if the mobility of polar groups at these sites differs, even if the "polarities" of the sites are equal. This gives the possibility of mapping binding sites in heterogeneous systems such as biological membranes.

References

Bakhshiev, N. G., Mazurenko, Y. T., & Piterskaya, I. V. (1966) *Opt. Spectrosc. (Engl. Transl.) 21*, 307.

Bevington, P. R. (1969) *Data Reduction and Error Analysis for the Physical Sciences*, McGraw-Hill, New York.

Brochon, J. C., & Wahl, Ph. (1972) *Eur. J. Biochem. 25*, 20.

Chakrabarti, S. K., & Ware, W. R. (1971) *J. Chem. Phys. 55*, 5494.

De Toma, R. P., & Brand, L. (1977) *Chem. Phys. Lett. 47*, 231.

De Toma, R. P., Easter, J. H., & Brand, L. (1976) *J. Am. Chem. Soc. 98*, 5001.

Easter, J. H., De Toma, R. P., & Brand, L. (1976) *Biophys. J. 16*, 571.

Fleming, P. J., Koppel, D. E., Lau, A. L. Y., & Strittmater, P. (1979) *Biochemistry 18*, 5458.

Gafni, A., De Toma, R. P., Manrow, R. E., & Brand, L. (1977) *Biophys. J. 17*, 155.

Ghiggino, K. P., Roberts, A. J., & Phillips, D. (1980) *J. Phys. E 13*, 446.

Grinvald, A., & Steinberg, I. Z. (1974) *Anal. Biochem. 59*, 583.

Haas, E., Katchalski-Katzir, E., & Steinberg, I. Z. (1978) *Biopolymers 17*, 11.

Halliday, L. A., & Topp, M. R. (1978) *J. Phys. Chem. 82*, 2415.

Ikkai, T., Wahl, Ph., & Auchet, J. C. (1979) *Eur. J. Biochem. 93*, 397.

Lee, A. G. (1978) *Recept. Recognition, Ser. A 5*, 81.

Leherer, S. S., Graceffa, P., & Betteridge, D. (1981) *Ann. N.Y. Acad. Sci.* (in press).

Li, Y. H., Chan, L.-M., Tyer, L., Moody, R. T., Himel, C. M., & Hercules, D. M. (1975) *J. Am. Chem. Soc. 97*, 3118.

Lipinski, J., Chojnacki, H., Grabowski, Z. R., & Rotkiewicz, K. (1980) *Chem. Phys. Lett. 70*, 449.

Marsh, D. J., & Lowey, S. (1980) *Biochemistry 19*, 774.

Mataga, N. (1963) *Bull. Chem. Soc. Jpn. 36*, 654.

McKinnon, A. E., Szabo, A. G., & Miller, D. R. (1977) *J. Phys. Chem. 81*, 1564.

Meech, S. R., O'Connor, D. V., Roberts, A. J., & Phillips, D. (1981) *Photochem. Photobiol. 33*, 159.

Michaelson, D. M., Horwitz, A. F., & Klein, M. P. (1974) *Biochemistry 13*, 2605.

Nishimoto, K. (1966) *Bull. Chem. Soc. Jpn. 39*, 645.
Nishimoto, K., & Fujishiro, R. (1964) *Bull. Chem. Soc. Jpn. 37*, 1660.
O'Connor, D. V., Ware, W. R., & Andre, J. C. (1979) *J. Phys. Chem. 83*, 1333.
Rapp, W., Klingenberg, H.-H., & Lessing, H. E. (1971) *Ber. Bunsenges. Phys. Chem. 75*, 883.
Stoffel, W., Tunggal, B. D., Zierenberg, O., Schreiber, E., & Binizek, E. (1974) *Hoppe-Seyler's Z. Physiol. Chem. 355*, 1367.
Tawada, K., Wahl, Ph., & Auchet, J. C. (1978) *Eur. J. Biochem. 88*, 411.
Wahl, Ph., Auchet, J. C., & Donzel, B. (1974) *Rev. Sci. Instrum. 45*, 28.
Wahl, Ph., Tawada, K., & Auchet, J. C. (1978) *Eur. J. Biochem. 88*, 421.
Ware, W. R., Lee, S. K., Brant, G. J., & Chow, P. P. (1971) *J. Chem. Phys. 54*, 4729.
Ware, W. R., Doemeny, L. J., & Nemzek, T. L. (1973) *J. Phys. Chem. 77*, 2038.

Intracellular pH Measurements by ^{31}P Nuclear Magnetic Resonance. Influence of Factors Other Than pH on ^{31}P Chemical Shifts†

Justin K. M. Roberts,‡ Norma Wade-Jardetzky,§ and Oleg Jardetzky*,§

ABSTRACT: Titration curves plotting chemical shift vs. pH for inorganic phosphate and glucose 6-phosphate in solutions of various composition are presented. Physiological concentrations of K^+ (0.1 M) and Mg^{2+} (5 mM) are shown to significantly shift the titration curve. The Mg^{2+} effect can be partly or completely reversed by addition of sufficient quantities of adenosine triphosphate or organic acids. The acidic protein bovine serum albumin and soluble maize root tip protein have no noticeable effect on the titration curves, whereas the basic protein protamine exerts a profound effect. The results clearly indicate that knowledge of intracellular ionic strength and free Mg^{2+} concentrations in the sample are required if the determination of intracellular pH by ^{31}P NMR is to be considered accurate within ±0.05–0.1 pH unit.

Since 1973 (Moon & Richards, 1973) in vivo ^{31}P nuclear magnetic resonance has been increasingly and extensively used to estimate intracellular pH [see Burt et al. (1979) and Radda & Seeley (1979) for reviews]. The method relies on the fact that the chemical shift (δ, resonance frequency relative to a standard) of ^{31}P in many phosphates is strongly dependent on pH; if the titration curve of a given phosphate compound in the intracellular milieu is known, a determination of pH from a measured δ is possible. Inorganic phosphate (P_i) and sugar phosphate resonances are the most suitable for measurement of intracellular pH (Burt et al., 1976), because their pK_a's lie near neutrality, and they are often present at high intracellular concentrations. The accuracy of the pH measurement (disregarding limitations imposed by the quality of the spectrum) depends on our understanding the extent to which factors other than pH influence δ. Analogous problems apply to other methods for measuring intracellular pH (Radda & Seeley, 1979).

The majority of articles describing application of the NMR method either fail to discuss whether or not factors other than pH affect the δ of P_i or state that factors such as Mg^{2+} (Burt et al., 1976, 1979; Navon et al., 1979; Colman & Gadian, 1976; Hollis, 1980) and ionic strength (Burt et al., 1976, 1979; Hollis, 1980) have no effect on the titration curve of P_i or that the effects can be ignored.

Recently an effect of ionic strength has been reported (Gadian et al., 1979; Ugurbil et al., 1979; Ogawa et al., 1978); we also reported (Roberts et al., 1980) that Mg^{2+} and certain concentrated polyelectrolytes shift the apparent pK_a of P_i.

Here we describe details of these and other effects, for both P_i and glucose 6-phosphate (Glc-6-P). Two observations indicate that at least some of these effects are significant: first, titration of P_i in undiluted, filtered homogenates of maize tissue (root tips or coleoptiles plus primary leaf) yield points that clearly do not lie on the titration curve of 5 mM KP_i. Second, when the cytoplasmic pH of maize root tip cells was induced to fall, the δ for the Glc-6-P resonance indicated a slightly larger drop (0.1 pH unit) than that indicated by the cytoplasmic P_i resonance, suggesting that one or both of the titration curves we were using to estimate pH did not exactly apply to the cytoplasm of these cells (unpublished results).

Materials and Methods

Preparation of Homogenates. Maize (*Zea mays* L.) root tips (1 mm long) from 2-day-old plants or coleoptiles and primary leaves from 4-day-old dark-grown plants were collected on ice, and ground in an ice-cold mortar. The homogenate was filtered through two layers of miracloth to remove the largest particles and so minimize suspension effects in the pH measurement using electrodes (Westcott, 1978). The pH was adjusted with 0.5 M NaOH or HCl.

Titration of P_i and Glc-6-P ^{31}P δ's. Although titration curves for P_i and Glc-6-P are plotted together, they were titrated as separate solutions—except those involving protamine and phospholipids. At least two solutions, separately made up, were titrated for each mixture. The pH was adjusted either by mixing different proportions of K_2HPO_4 and KH_2PO_4 solutions or by adding 0.5 M NaOH or HCl. Protamine (free base) was acidified with concentrated HCl.

Potentiometric Titrations. Potassium phosphate or Na_2Glc-6-P (100 mL, 5 mM) was adjusted to pH 2.5–3.0 with 0.5 M HCl, and titrated with 0.5 M NaOH, the pH being

† From the Stanford Magnetic Resonance Laboratory, Stanford University, Stanford, California 94305. *Received November 3, 1980; revised manuscript received May 27, 1981.* This research was supported by grants from the National Science Foundation (PCM7809230, PCM7807930, and GP23633) and the National Institutes of Health (RR00711).
‡ Department of Biological Sciences, Stanford University.
§ Stanford Magnetic Resonance Laboratory.

0006-2960/81/0420-5389$01.25/0